JUNE 2009

SolidState TECHNOLOGY®

THE INTERNATIONAL MAGAZINE FOR SEMICONDUCTOR MANUFACTURING

Thin films for 3D p. 12

- Measuring monolayer graphite with reflectometry-ellipsometry p. 18
- ODP metrology with floating *n*&*k*'s p. 22
- Camera-phone optics p. 26

www.solid-state.com

Incorporating Advanced Packaging

MATERIALS

Combined reflectometry-ellipsometry technique to measure graphite down to monolayer thickness

EXECUTIVE OVERVIEW Graphene, the single layer of graphite, has been the focus of many researchers internationally because of its unique electronic properties. The characterization of graphene films deposited on various substrates other than SiO_2 has been a challenging task thus far. This article discusses a rapid, sensitive, and non-destructive method for characterization of graphene on various substrates, including silicon, based on combined reflectometry and ellipsometry techniques. The optical properties deduced from the multi-angle, polarized light measurements in the range of 190–1000nm suggest that multi-layer graphite is a birefringent material with thickness-dependent optical properties.

Graphene, a one-atom-thick planar sheet of SP2-bonded carbon atoms densely packed in a honeycomb crystal lattice, has attracted interest since the first reports of experiments on the stand-alone, single-layer crystal in 2004 [1,2]. Graphene is the basic structural element of all graphitic materials including graphite, fullerenes, and carbon nanotubes (CNTs). Free-standing graphene sheets have exhibited remarkably high carrier mobility at room temperature, which makes it promising for applications in ultra-high-frequency signal processing and for chemical or bio-chemical sensing.

Intrinsic graphene sheet is a semi-metal or zero-gap semiconductor. In its nanoribbon (GNR) form, however, with a width on the order of nanometers, graphene exhibits a bandgap due to quantum confinement effects. The bandgap depends on the nanoribbon orientation relative to the graphene crystal structure; both semiconducting and metallic properties can be achieved by armchair GNR and zigzag GNR [3,4] structures, respectively.

Recently, FET-type devices based on armchair GNR have been studied experimentally [5] and theoretically [6]. Quantum dot (QD) devices can also be made entirely from graphene, including central islands (CIs), quantum barriers, source/drain contacts, and side-gate electrodes [7]. Due to the high transparency of graphene, it has been used as a conductive electrode for LCD displays and solar cells [8]. Finally, graphene sheet exhibits a spring constant on the order of 1–5N/m with a Young's modulus of ~0.5TPa. These remarkable mechanical properties make graphene a candidate for use in such MEMS applications as pressure sensors and resonators [9].

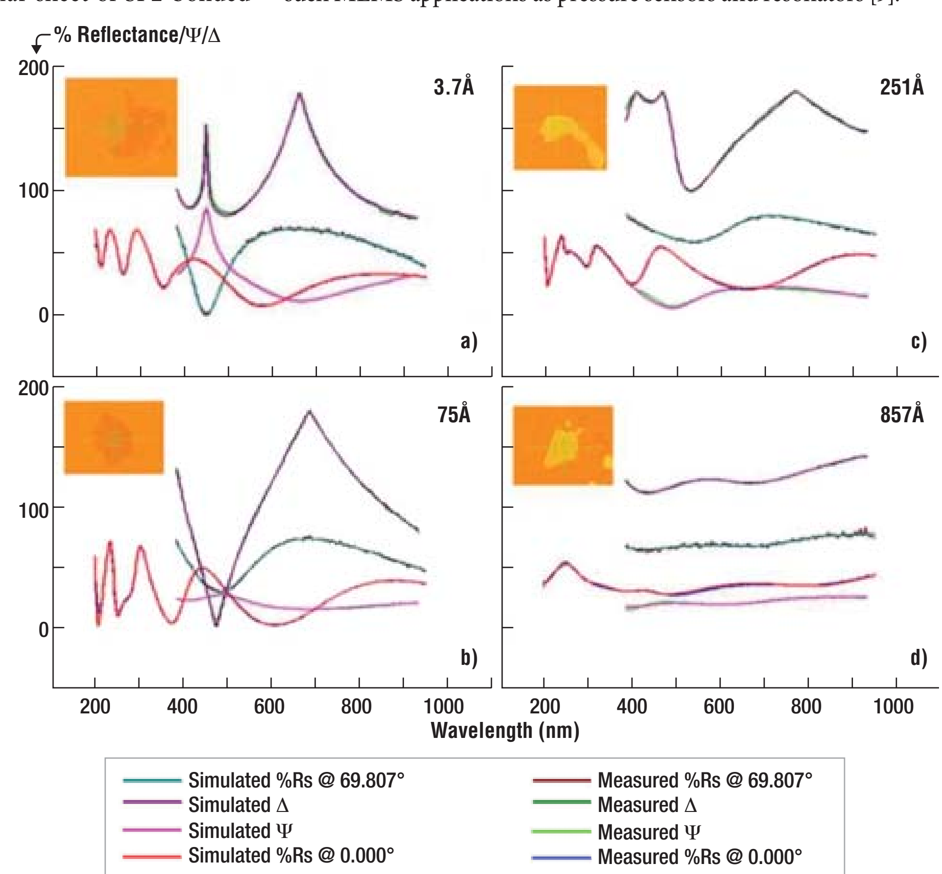

Figure 1. The multi-angle reflectance and ellipsometric data and analysis obtained for different graphite flake thicknesses on a 300nm SiO_2 film grown on a silicon substrate.

Wei-E Wang, Intel Corp. c/o IMEC, Leuven, Belgium; **M. Balooch**, UC Berkeley, CA USA; **C. Claypool**, **M. Zawaideh**, **K. Farnaam**, Scientific Computing International, Carlsbad, CA USA

A monolayer of graphene with 0.34nm thickness is invisible to optical microscopes unless it is deposited on a well-chosen 300nm-thick layer of SiO_2 grown on a Si substrate. This allows multi-layer light interference to provide enough contrast to observe a single graphene layer flake relative to the surrounding oxide. Even for such a case, the graphite thickness cannot be determined by simple examination under the optical microscope. Atomic force microscopy is an option for quantitative measurements, though it has low throughput and could damage the crystal lattice.

It has been reported that a broadband, near-normal incidence reflectometry technique can quantitatively measure graphene and graphite thickness deposited on a layer of ~300nm of SiO_2 grown on a Si substrate [10]. A single complex index of refraction as a function of wavelength was sufficient for measuring all graphite thicknesses down to monolayer graphene. A corresponding simulation also suggested that the technique can be applied to other substrates, such as epitaxial growth on SiC and catalytic surfaces as Ni or Pt [10]. When graphene is deposited directly on silicon (Si), reflectometry cannot provide enough sensitivity for adequate film characterization.

Here, the study is extended with a combination of multiple-angle reflectometry and grazing angle spectroscopic ellipsometry. This combination characterizes graphene on essentially any substrate material. The thin graphite films (i.e., multi-layer graphene) were found to exhibit optical birefringence. Birefringent materials are widely used in optical devices, such as LCDs, light modulators, color filters, wave plates, optical axis gratings, and optical pickup [11]. Birefringence also plays impacts second harmonic generation and other nonlinear processes.

Theory and method

Reflectometry and ellipsometry measure the thickness and optical constants (refractive index n and extinction coefficient k) of thin films. Both are based on detecting changes in reflected or transmitted light from a sample to deduce its properties: reflectometry relies on intensity changes in the reflected light; ellipsometry relies on polarization changes. In ellipsometry, the component waves of the incident light, which are linearly polarized with the electric field vibrating parallel (p or TM) or perpendicular (s or TE) to the plane of incidence, experience different amplitude attenuations and absolute phase shifts upon reflection. The ellipsometry measurement is often expressed as the complex ratio of polarization states $\rho\ \frac{r_p}{r_s} = \rho := \tan \Psi\ e^{i\Delta}$ as an amplitude $\tan\psi$ and a phase Δ. Ellipsometry derives its sensitivity from the fact that the polarization-altering properties of the reflecting boundary are modified significantly even when ultra-thin films are present. Given either intensities or polarization states for the incident and reflected beams, the film properties can be calculated using appropriate models and dispersion equations to match the measured optical response.

Using a general dispersion model that covers the entire wavelength range of the measurement, the number of variables or parameters required to model optical response is reduced, eliminating the potential for multiple solutions. This approach allows the user to model complex multilayer structures with reflection and ellipsometric data. Several common analytical expressions for $n(\lambda)$ and

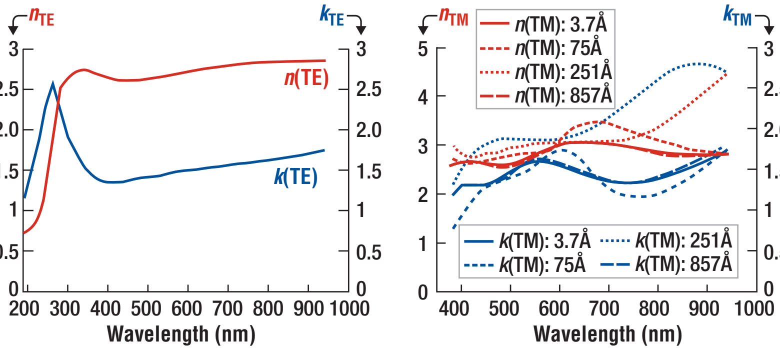

Figure 2. n&k variation with wavelength for TE (thickness independent) and TM (thickness dependent) polarizations.

$k(\lambda)$ are commonly used, such as the Sellmeier or Cauchy dispersion relations; however, the more robust choices of index dispersion are obtained by ensuring that $n(\lambda)$ and $k(\lambda)$ obey Kramers-Kronig (KK) relation. The KK relation, derived from a causality principle of electromagnetic wave propagation, specifies that if the imaginary part of the index is known over all energies, the real part is uniquely determined through $n(E) - 1 = \frac{2}{\pi} P \int_0^{\infty} \frac{\xi k(\xi)}{\xi^2 - E^2} d\xi$ where P is the Cauchy

Combined reflectometry-ellipsometry technique *continued from page 19*

principal value of the integral [12]. As a special case of the KK relation, one can show that the popular Cauchy index dispersion satisfies it, but only in the region far enough from energies where absorption occurs in the material.

A KK-consistent dispersion relation is produced by modeling the absorption in the material from fundamental physical principles and then deriving an expression for the real part of the index from the equation above. A KK-consistent dispersion relation, the Tauc-Lorentz (TL) expression, was successfully used in modeling experimentally measured optical constants of amorphous dielectrics, polymers, and semiconductor materials. This expression convolves Lorentz absorption of isolated oscillators with the Tauc joint density of states [13]. The TL model approximates k near the band gap as a quadratic function of energy; however, k is forced to 0 for photon energies less than the band gap.

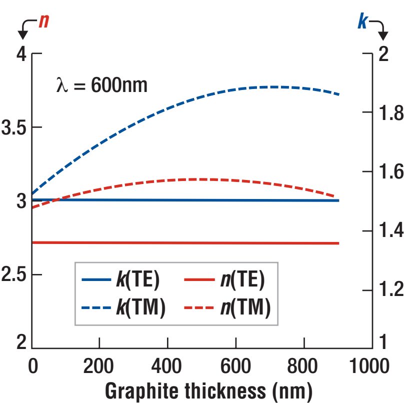

Figure 3. The variation of n and k (TM polarization) with graphite thickness at 600nm.

Another KK-consistent dispersion relation, the Scientific Computing International (SCI) model [14], is based on Lorentz absorption of isolated oscillators and an improvement over the TL model. SCI's dispersion formula treats k near the band gap with a high order polynomial approximation that is significantly closer to the physical solution. As with the Tauc-Lorentz model, k is forced to 0 when the photon energy is less than the band gap. However, the extinction coefficient is allowed to be non-zero for photon energies much less than the band gap energy, which allows for modeling materials with absorption in the NIR.

Simultaneous reflection measurements at normal to the surface (0°) and oblique (70°) angles, along with the phase (Δ) and amplitude ratio (Ψ) values obtained from grazing angle ellipsometric measurements assures an unambiguous and accurate determination of thin film properties on most substrates.

Characterization of <20Å films on bulk substrates using conventional reflectometry techniques is a challenging task as, with decreasing thickness, the optical response of the film is diminished and the small signal change often gets buried in the noise [10]. Researchers have circumvented the problem by sandwiching an oxide layer of ~300nm of SiO_2 between the substrate and the thin film to take advantage of the effect of multiple internal reflections. However, in practice, many thin-film devices require their own substrate materials. We collected multiple-angle, polarized reflection measurements of the graphite flakes deposited on 300nm of SiO_2 on Si, which provides the detailed optical properties of the graphene in addition to film thickness. Once the graphene optical properties are accurately determined, detection of graphene monolayer films can be made with confidence on almost any substrate.

The FilmTek 4000EM-DUV used to measure and analyze the graphene flakes is a fiber-optics-based system with a tungsten/deuterium light source and fixed-grating CCD-array spectrometers. The ellipsometer is a rotating compensator design [15] that results in a high signal-to-noise ratio, particularly important for thin film detection. Absolute reflection spectra are obtained by collecting reflection spectra from the sample of interest in ratio to reflection spectra from a known sample (i.e., bare Si). Reflection and ellipsometric spectra can be measured from deep-UV to near-IR, with acquisition time taking a few seconds. Various optical configurations allow for a 3.5mm–40µm measurement spot size.

Special software simultaneously solves for refractive index $n(\lambda)$, extinction coefficient $k(\lambda)$, and thicknesses of multilayer film structures. A self-consistent solution is obtained using the SCI generalized dispersion formula to model fitted values of the dielectric function $\varepsilon(\lambda)$ to the measured reflection and ellipsometry data. Global-optimization methods help obtain the best solution while avoiding local minima and minimizing sensitivity to the user's initial guess of fitted parameters. The software optimizes the reflection, ellipsometric, and the power-density-spectrum (fast-Fourier-transform) data simultaneously. This enables accurate thickness determination from 0 to 350µm.

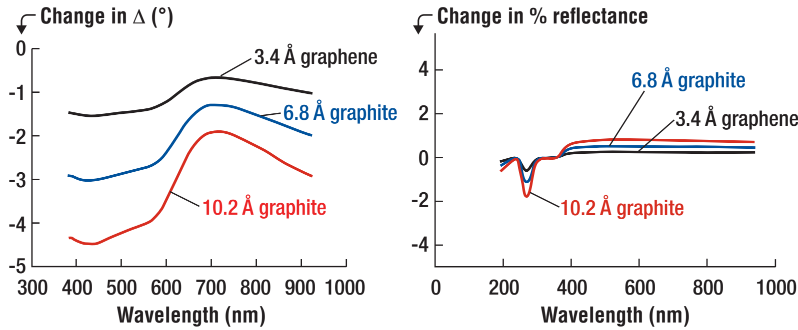

Figure 4. Simulated graphs showing the sensitivity of Δ and % reflectance vs. wavelength for 1, 2, and 3 monolayers of graphene on a Si substrate.

Measurement results

A sample with numerous flakes of graphite having different thickness on 300nm of SiO_2 on a Si substrate was prepared by Graphene Industries Limited (Manchester, UK). The sample investigated in the present work is the same as that used in previous reflectometry studies [10]. The coordinate was given for a flake of $75 \times 50\mu m^2$ graphene. **Figure 1a** shows the optical image containing a graphene flake that is not clearly visible; multi-layer flakes, however, are optically visible as shown in Figs. 1b-1d for a few selected flakes.

Multiple-angle, polarized reflectance measurements were performed using a FilmTek 4000EM-DUV. The experimental and simulated values of multi-angle reflectance, Δ and Ψ, are shown in these figures. The incident beam diameters are overlapped within a 40 × 40µm spot. The normal incidence broadband reflectance spectrum was collected in the 190–1000nm wavelength range, and the 70° reflectance and ellipsometric spectra were collected in the 380–1000nm range. Both the normal incidence and grazing angle reflectance data were collected for TE polarization. All spectra were

analyzed using SCI's proprietary dispersion relations and global optimization methods to simultaneously determine the graphene flake thickness and optical constants. Literature values for the optical properties of Si and SiO_2 [16] were used in the data analysis.

The complex index of refraction of graphite has been reported in the literature using optical, photoemission, and EELS methods [17-21]. In fact, the graphene index of refraction for TE polarization obtained from the multi-angle polarized reflection data is in agreement with previous TE index values for graphite [17]. Additionally, the anisotropy of the graphene film can be determined by including the spectroscopic ellipsometric data in the analysis. Although previous measurements indicated that graphite is birefringent, the reported values for the TM index of refraction have varied greatly.

The resultant real index of refraction *(n)* and extinction coefficient *(k)* as functions of wavelength are shown in **Fig. 2.** The TE index of refraction appears to be independent of graphite thickness down to one monolayer. However, *n* and *k* vary with graphite thickness for TM polarization, suggesting that graphene birefringence changes with thickness. The variation of *n* and *k* for TM polarization is appreciable with graphite thickness at a wavelength of 600nm **(Fig. 3).**

Although optical microscopy provides sufficient contrast and reflectometry to measure graphite thickness down to a monolayer on SiO_2, using an oxide layer of certain thickness limits the applicability of both techniques. Graphene measurementon different substrates demands a more reliable approach. Combined multi-angle reflectometry and ellipsometry can conveniently perform graphene measurements on a variety of substrates.

The ellipsometric data suits measuring very thin layers of graphene. In the simulated results for graphene on Si **(Fig. 4),** changes in Δ for 1, 2, and 3 monolayers of graphene on a Si substrate are plotted versus wavelength. The simulation was performed to demonstrate that such films can be measured once the samples are obtained. The change in Δ is about 1.5° at 425nm for each additional graphene layer, well over an order of magnitude higher than the sensitivity limit of the tool (~0.02°). Contrast this with the change in reflection, which is quite small, considering the average noise in the reflectance measurements is about ~0.1%, only a factor of 4 lower than the change in reflection due to the graphene layers. Combined data collection ensures unambiguous detection of graphene on Si.

Conclusion

The accurate optical properties for graphene and graphite were determined in the 190–1000nm wavelength range using multi-layer graphite flakes on a substrate comprising bulk Si and a 300nm SiO_2 film. These optical properties are derived as a function of thickness of graphite for TE and TM polarizations of light. The results suggest the complex index of refraction for TE is independent of thickness down to one monolayer (i.e., graphene). However, the index varies appreciably for TM polarization with thickness, suggesting the graphite birefringence is dependent on film thickness. It is also concluded that the integrated broadband, multi-angle reflectometry-ellipsometry technique has the capability to detect graphene on essentially any substrate. ■

References

1. K. S. Novoselov, A. K. Geim, S. V. Morozov, D. Jiang, Y. Zhang, S. V.Dubonos, I. V. Grigorieva, and A. A. Firsov, *Science* 306, 666 (2004).
2. A. K. Geim and K. S. Novoselov, *Nat. Mater.* 6, 183 (2007).
3. M. Fujita, K. Wakabayashi, K. Nakada, and K. Kusakabe, "Peculiar localized state at zigzag graphite edge," *Journal of the Physical Society of Japan,* vol. 65, pp. 1920-1923, July 1996.
4. G.-C. Liang, N. Neophytos, D. Nikonov, and M. Lundstrom, "Performance projections for ballistic graphene nanoribbon field-effect transistors," *IEEE Transactions on Electron Devices,* vol. 54 (4) 677 - 682, April 2007.
5. C. Berger, Z. Song, X. Li1, X. Wu, N. Brown, C. Naud, D. Mayou, T. Li, J. Hass, A. N. Marchenkov, E. H. Conrad, P. N. First and W.A. de Heer, "Electronic Confinement and Coherence in Patterned Epitaxial Graphene," *Science,* vol. 312, pp. 1191-1196, May 2006.
6. G.-C. Liang, N. Neophytou, D. Nikonov, and M. Lundstrom "Theoretical Study of Graphene Nanoribbon Field-Effect Transistors," Proceeding of Conference, Nanotech 2007, May 2007.
7. L. A. Ponomarenko, F. Schedin, M. I. Katsnelson, R. Yang, E. W. Hill, K. S. Novoselov, and A. K. Geim "Chaotic Dirac Billiard in Graphene Quantum Dots" *Science* vol. 320, 356 (2008).
8. Frank, I. W., Tanenbaum, D. M., Van Der Zande, A.M., and McEuen, P. L. Mechanical Properties of Suspended Graphene Sheets. *J. Vac. Sci. Technol. B* 25, 2558-2561 (2007)
9. T. Pichler, "Molecular Nanostructures: Carbon Ahead," *Nature Materials*, vol. 6, 332 (2007).
10. A. Gray, M. Balooch, S. Allegret, S. De Gendt and W.E. Wang, *J. Appl. Phys.*, 104,053109 (2008)
11. K. Kinnstatter, M. Ojima, and S. Yonezawa, *App. Opt.* 29, 4408 (1990).
12. J. D. Jackson, "Classical Electrodynamics," John Wiley and Sons, New York (1975), p. 311.
13. G. E. Jellison, Jr, and F. A. Modine, "Parameterization of the optical functions of amorphous materials in the interband region," *Appl. Phys. Lett.* 69, 371-373 (1996).
14. E. Zawaideh, U. S. Patent 5,889,592 (1999)
15. P. S. Hauge, "Generalized Rotating-Compensator Ellipsometry," *Surface Science,* 56, 148 (1976).
16. E. D. Palik, *Handbook of Optical Constants of Solids I,* Academic Press, Orlando, (1985).
17. E. D. Palik, *Handbook of Optical Constants of Solids II,* Academic Press, Boston, (1991).
18. F. Bassani and E. Tosatti, *Phys. Lett. A* 27, 446 (1968).
19. T. G. Pedesen, *Phys. Rev. B* 67, 113106 (2003)
20. L. A. Falkovsky and A. A. Varlamov, *Eur. Phys. J. B* 56, 281 (2007)
21. J. Nillson et al, *Phys. Rev. Lett.* 97, 266801 (2006).

Acknowledgment

The authors thank Stephane Allegret and Stefan De Gendt of IMEC. FilmTek is a trademark of Scientific Computing International.

WEI-E WANG received his PhD from the U. of California at Berkeley and is currently an Intel assignee to *IMEC, Kapeldreef 75, B-3001 Leuven, Belgium*; ph.: +32-1628-7891; weie.want@intel.com.

MEHDI BALOOCH received his PhD in physical chemistry from MIT and is a senior research scientist at *UC-Berkeley, Berkeley, CA USA.*

CHRIS CLAYPOOL received his PhD in physical chemistry from the California Institute of Technology and is CTO at *Scientific Computing International, Carlsbad, CA USA.*

MAZEN ZAWAIDEH is a student at UC San Diego and interning at *Scientific Computing International.*

KAMBIZ FARNAAM received his PhD in materials from UC Berkeley and is VP of marketing at *Scientific Computing International.*